THE JOURNAL OF BIOLOGICAL CHEMISTRY VOL. 289, NO. 28, pp. 19714–19725, July 11, 2014
© 2014 by The American Society for Biochemistry and Molecular Biology, Inc. Published in the U.S.A.

Endoplasmic Reticulum-associated Degradation of Niemann-Pick C1

*EVIDENCE FOR THE ROLE OF HEAT SHOCK PROTEINS AND IDENTIFICATION OF LYSINE RESIDUES THAT ACCEPT UBIQUITIN**

Received for publication, January 12, 2014, and in revised form, May 22, 2014 Published, JBC Papers in Press, June 2, 2014, DOI 10.1074/jbc.M114.549915

Naoe Nakasone[‡], **Yuko S. Nakamura**[§], **Katsumi Higaki**[¶], **Nao Oumi**[‖], **Kousaku Ohno**[**], **and Haruaki Ninomiya**[‡1]

From the Departments of [‡]Biological Regulations and [**]Child Neurology, Tottori University Faculty of Medicine, Yonago 683-8503, [§]Applied Biotechnology, Tottori Institute of Industrial Technology, Yonago 684-0041, the [¶]Division of Functional Genomics, Research Center for Bioscience and Technology, Tottori University, Yonago 683-8503, and the [‖]Tottori University Hospital Cancer Center, Yonago 683-8504, Japan

Background: Mutant Niemann-Pick C1 (NPC1) is degraded by the proteasome.
Results: NPC1 is one of the clients of HSP/CHIP (heat shock protein/carboxyl terminus of Hsp70-interacting protein) complexes and accepts ubiquitin at multiple lysine residues.
Conclusion: HSPs are critical in the quality control of NPC1.
Significance: Unraveling the mechanisms of NPC1 degradation is crucial for development of a chaperone therapy.

Most cases with Niemann-Pick disease type C carry mutations in *NPC1*. Some of the mutations, including the most frequent I1061T, give rise to unstable proteins selected for endoplasmic reticulum-associated degradation. The purpose of the current study was to shed mechanistic insights into the degradation process. A proteasome inhibitor MG132 prolonged the life span of the wild-type NPC1 expressed in COS cells. The expressed protein associated with multiple chaperones including heat shock protein 90 (Hsp90), Hsp70, heat shock cognate protein 70 (Hsc70), and calnexin. Accordingly, expression of an E3 ligase CHIP (carboxyl terminus of Hsp70-interacting protein) enhanced MG132-induced accumulation of ubiquitylated NPC1. Co-expression and RNAi knockdown experiments in HEK cells indicated that Hsp70/Hsp90 stabilized NPC1, whereas Hsc70 destabilized it. In human fibroblasts carrying the I1061T mutation, adenovirus-mediated expression of Hsp70 or treatment with an HSP-inducer geranylgeranylacetone (GGA) increased the level of the mutant protein. In GGA-treated cells, the rescued protein was localized in the late endosome and ameliorated cholesterol accumulation. MALDI-TOF mass spectrometry revealed three lysine residues at amino acids 318, 792, and 1180 as potential ubiquitin-conjugation sites. Substitutions of the three residues with alanine yielded a mutant protein with a steady-state level more than three times higher than that of the wild-type. Introduction of the same substitutions to the I1061T mutant resulted in an increase in its protein level and functional restoration. These findings indicated the role of HSPs in quality control of NPC1 and revealed the role of three lysine residues as ubiquitin-conjugation sites.

Niemann-Pick disease type C (NPC)[2] is an autosomal recessive lipid storage disorder characterized by an accumulation of free cholesterol and other lipids in the late endosome/lysosome (1). It is caused by mutations in *NPC1* or *NPC2* genes (2, 3). NPC1 is a membrane protein that resides primarily in the late endosome, whereas NPC2 is a soluble protein that resides primarily in the lysosome (4, 5). 95% of NPC patients carry mutations in the *NPC1* gene, and more than 200 mutations of *NPC1* responsible for NPC have been identified. Some of the mutations are predicted to cause premature termination or large deletion of the polypeptide, but many others are predicted to cause single amino acid substitution or small in-frame deletion, including the most frequent I1061T substitution that is found in ~20% of disease alleles (6).

We and others (7–9) reported reduced protein levels of NPC1 in fibroblasts from patients with *NPC1* mutations. Importantly, cells from patients with juvenile/adult forms retained relatively high levels of the protein (7), suggesting that the NPC1 protein level may be one of the major factors that determine disease severity. It was unlikely that this decrease was secondary to any cellular phenotype of NPC, because NPC2-deficient cells contained increased levels of NPC1 (7, 8) and also because treatment of the cells with U18666A that induces an NPC phenotype increased the NPC1 protein level (10). We found rather increased levels of NPC1 mRNA in these cells (11), excluding the possibility that the decreased protein level was attributable to impaired transcription.

Gelsthorpe *et al.* (9) reported that treatment of I1061T homozygous human fibroblasts with chemical chaperones (*i.e.* glycerol or 4-phenylbutyric acid) increased the protein level of the mutant NPC1 and that overexpression of the I1061T

* This work was supported in part by a research grant from Ara Parseghian Medical Research Foundation (to H. N.).
[1] To whom correspondence should be addressed. Tel.: 81-859-38-6351; Fax: 81-859-38-6350; E-mail: ninomiya@med.tottori-u.ac.jp.

[2] The abbreviations used are: NPC, Niemann-Pick C; ERAD, endoplasmic reticulum-associated degradation; Insig-1, insulin induced gene-1; Hsc70, heat shock cognate protein 70; TPR, tetratricopeptide repeat; BAG2, BCL2-associated athanogene 2; IB, immunoblotting; IP, immunoprecipitation; GGA, geranylgeranylacetone.

mutant in NPC1-deficient CHO cells restored the cholesterol flow. They concluded that the I1061T mutant retains NPC1 function but is selected for endoplasmic reticulum-associated degradation (ERAD) due to protein misfolding. This conclusion was supported by subsequent studies that demonstrated the ability of ryanodine receptor antagonists (12) or MG132 (13) to increase the protein level of the I1061T mutant and alleviate cholesterol accumulation in patient-derived cells. Recently, Ohgane *et al.* (14) described oxysterol derivatives that could bind to and suppress degradation of this mutant protein. Despite these lines of evidence for NPC1 ERAD, the quality control and degradation mechanisms at the molecular level remain largely unknown.

In ERAD, molecular chaperones play a critical role in the quality control of proteins, assisting their folding and also facilitating degradation of misfolded polypeptides by the ubiquitin-proteasome system. Proteins are earmarked for degradation by the covalent attachment of a polyubiquitin chain(s) to a lysine residue(s). This is a multistep process involving an E1 ubiquitin-activating enzyme, E2 ubiquitin-conjugating enzyme, and E3 ubiquitin ligase (15, 16). The purpose of the current study was to shed mechanistic insights to the NPC1 ERAD. Specifically, we aimed at identification of molecular chaperones that participate in quality control of NPC1 and lysine residues that accept ubiquitin.

EXPERIMENTAL PROCEDURES

Materials—Dulbecco's modified Eagle's medium and Ham's F-12 medium were from Invitrogen. Bovine calf serum was from Atlanta Biologicals. Geldanamycin, anti-FLAG M2-agarose, and rabbit polyclonal anti-FLAG were from Sigma. Rabbit polyclonal antibody against NPC1 was from Abcam and against Insig-1 (insulin-induced gene-1) from Biorbyt. Mouse monoclonal antibodies against ubiquitin (P4D1), heat shock protein 40 (Hsp40), Hsp70, Hsp90, heat shock cognate protein 70 (Hsc70), calnexin, HA tag, and GFP and rabbit polyclonal antibody against CHIP (carboxyl terminus of Hsp70-interacting protein) were from Santa Cruz Biotechnology. Geranylgeranylacetone was a gift from Eisai Co., Ltd. (Tokyo, Japan).

Expression of Recombinant Proteins and RNAi Knockdown of Endogenous Proteins—All expression plasmids encoded human proteins and all siRNAs were based on human sequences. pASC9/FLAG-NPC1, an expression plasmid of NPC1 with a FLAG tag in the ClaI site, has been described (17). pSV-SPORT/NPC1 wild-type and mutants with amino acid substitutions Y634C, P691S, or I1061T were a gift from Dr. J. F. Strauss III (University of Pennsylvania Medical Center). The PsyI fragment of the FLAG-NPC1 cDNA that flanks the FLAG epitope was introduced to the corresponding site of pSV-SPORT/NPC1 to generate a FLAG-tagged version of the cDNAs. The carboxyl-terminal 12 base pairs were deleted from pSV-SPORT/FLAG-NPC1 by PCR-based mutagenesis to generate a cDNA that encoded FLAG-NPC1/δLLNF. Lysine residues at amino acids 318, 792, and 1180 were substituted by alanine using a QuikChange Site-directed mutagenesis kit (Stratagene) and the substitution was confirmed by direct sequencing. pcDNA3.1 expression plasmids of Hsc70, Hsp70, and Hsp90 have been described (18) and those of FLAG-CHIP and CHIP/δTPR that lacked the tetratricopeptide repeat (TPR) domains were a gift from Dr. I. Hisatome (Tottori University). pcDNA3.1 plasmids of HA-BAG2 (BCL2-associated athanogene 2) and FLAG-gp78 were a gift from Dr. C. Patterson (University of North Carolina at Chapel Hill) and Dr. Y. Yihong (National Institutes of Health, NIDDK), respectively. siRNAs against Hsc70 and Hsp70 have been described (18). The sequence of siRNA against CHIP was: *sense,* 5′-GGAGCAGGGCAAUCGUCUGTT-3′, and *antisense,* 5′-CAGACGAUUGCCCUGCUCCTT-3′. COS or HEK cells were transfected with the expression plasmid or siRNA using Lipofectamine 2000 reagent (Invitrogen) according to the manufacturer's instructions. Adenoviruses carrying *LacZ* or *Hsp70* (19) were a gift from Dr. A. Nakai (Yamaguchi University).

Cell Culture—COS cells, HEK cells, and human skin fibroblasts were maintained in DMEM, 10% bovine calf serum at 37 °C in a humidified atmosphere with 5% CO_2. We used four lines of human skin fibroblasts, one from a control subject and three from NPC patients. The NPC1 mutations of the three patients were I1061T/I1061T, I1061T/del 740,741, and F705S/S813X. CHO/NPC1(−) cells that do not express NPC1 and CHO/FLAG-NPC1 knock-in cells that stably express FLAG-NPC1 (10) were maintained in the same way except for the use of F-12 medium instead of DMEM.

Immunocytochemistry and Filipin Staining—All procedures were carried out at 4 °C. For FLAG-NPC1 expression experiments using CHO/NPC1(−) cells, cells on coverslips were fixed with 4% paraformaldehyde in PBS for 15 min, permeabilized with 0.5% Nonidet P-40 in PBS for 15 min, blocked with 1% bovine serum albumin for 1 h, and incubated with rabbit anti-FLAG (1:200) for 1 h. Bound antibodies were detected with Alexa 548-conjugated secondary antibody. Filipin staining was performed as described (10) and images were obtained using Leica TSC SP-2 confocal laser microscope. For filipin staining of human skin fibroblasts, fixed cells were incubated with filipin in the same way and images were obtained using Leica DMRB fluorescent microscope. For quantification of fluorescent signals, the regions of interest was set to surround the perinuclear signals and the average intensity was obtained using NIH ImageJ software.

Immunoprecipitation and Western Blotting—All procedures were carried out at 4 °C. Cells were washed with PBS and lysed by sonication in buffer A (10 mM Tris-Cl, pH 7.4, 150 mM NaCl, 1 mM EDTA, 1 mM EGTA, 1% Triton X-100) supplemented with Complete protease inhibitor mixture (Roche Applied Science). After a brief centrifugation to remove insoluble material, the supernatant was precleared with an aliquot of agarose beads. For immunoprecipitation (IP) of FLAG-NPC1, the extracts were incubated for 16 h with anti-FLAG M2-agarose beads, washed with buffer A, and followed by elution of bound proteins by heating at 65 °C for 10 min in SDS-PAGE sample buffer. For IP of endogenous NPC1, the extracts were incubated for 16 h with anti-NPC1 and immune complexes were collected by using Dynabeads protein G (VERITAS). SDS-PAGE, Western transfer, and immunoblotting (IB) were carried out as described (10). The blot was developed using an ECL kit (Amersham Biosciences).

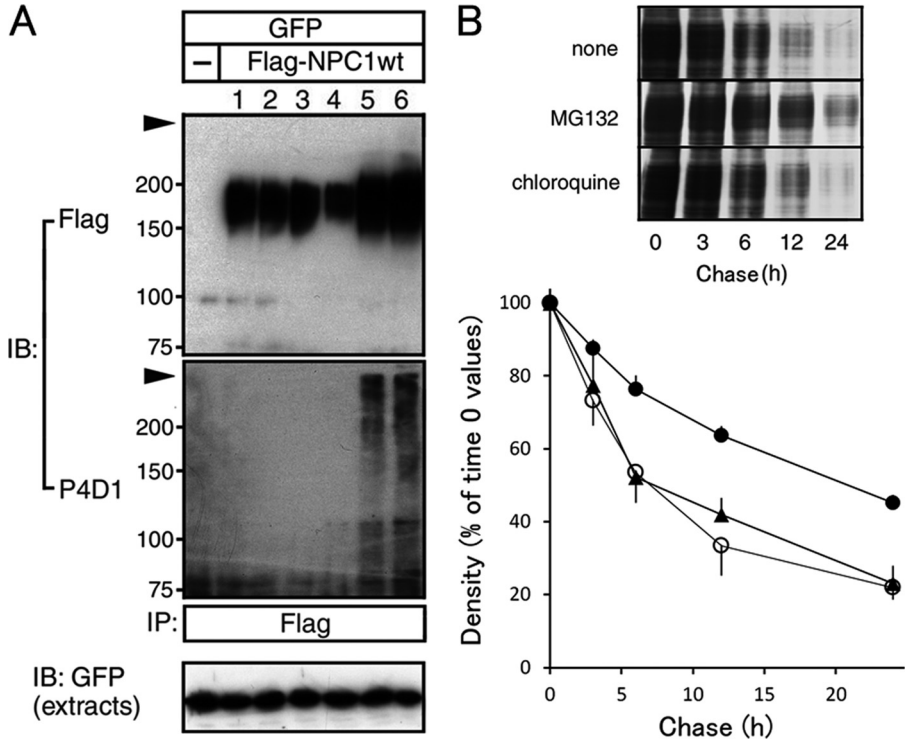

FIGURE 1. **Effects of protease inhibitors on expression and degradation of FLAG-NPC1.** *A*, levels of FLAG-NPC1 and its ubiquitylated form. COS cells were transfected with expression constructs for FLAG-NPC1 and GFP. At 48 h post-transfection, they were incubated for 6 h in the absence (*lane 1*) or presence of 0.15 mM chloroquine (*lane 2*), 0.1 mM leupeptine (*lane 3*), 10 mM NH_4Cl (*lane 4*), 5 μM MG132 (*lane 5*), or 5 μM lactacyctin (*lane 6*). 1% Triton X-100 extracts were subjected to anti-GFP IB or anti-FLAG IP. The IP products were probed with anti-FLAG or anti-ubiquitin (P4D1). Molecular masses are given on the *left* (kDa). The *arrowheads* indicate the top margin of the separating gel. Shown are representative results reproduced three times. *B*, degradation of FLAG-NPC1. Transfected cells were pulse-labeled with [^{35}S]Met/Cys and chased in the absence (*open circles*) or presence of 5 μM MG132 (*closed circles*) or 0.15 mM chloroquine (*triangles*). At the times indicated, cells were harvested and anti-FLAG IP products were subjected to autoradiography. Representative autoradiographs are shown. Band densities were determined by densitometry and expressed as relative to the values at time 0. Each *dot* represents mean ± S.E. of three determinations. $t_{1/2}$ values are given in the text.

Pulse-Chase Analysis—COS cells in 6-well plates were transfected with the indicated expression constructs. 48 h after transfection, cells were pulse-labeled for 2 h with EXPRESS^{TM} [^{35}S]Met/Cys (50 μCi/ml, PerkinElmer Life Sciences) in Met/Cys-free DMEM supplemented with dialyzed bovine calf serum and then chased in DMEM, 10% bovine calf serum. FLAG-NPC1 was immunoprecipitated from 1% Triton X-100 extracts and analyzed by SDS-PAGE followed by autoradiography. Densitometry was performed using NIH ImageJ software. The decay constant (k) was estimated by fitting first-order decay curves to form $y = e^{-kt}$ by using Excel software and a half-life time was calculated using the formula $t_{1/2} = 0.693/k$.

Cell Fractionation—Membranes were fractionated by using an Opti-prep gradient (Axis-Shield plc.) as described (20). Briefly, cells were homogenized with a Potter homogenizer in ice-cold buffer (10 mM Hepes, pH 7.0, 1 mM EDTA, 1 mM EGTA supplemented with a protease inhibitor mixture). After centrifugation at 100,000 × g for 1 h at 4 °C, the supernatant was discarded and the pellet was resuspended in the same buffer, overlaid onto an Opti-prep gradient, and centrifuged at 100,000 × g for 16 h at 4 °C. The top 12 fractions of the gradient were recovered and numbered accordingly.

MALDI-TOF Mass Spectrometry—CHO/FLAG-NPC1 knock-in cells were incubated in the absence or presence of 5 μM MG132 for 6 h and FLAG-NPC1 was recovered from cell extracts by anti-FLAG IP and subjected to SDS-PAGE. FLAG-NPC1 in excised gel plugs was digested using sequencing grade modified porcine trypsin. The peptides were extracted, dried in a vacuum, centrifuged, and redissolved in 0.1% trifluoroacetic acid. The peptide mixture resulted from protein digestion was analyzed using a Voyager-DE STR MALDI-TOF mass spectrometer (Applied Biosystems).

Statistical Analysis—Student's t test was used for statistical analysis of the results. p values of <0.05 were considered to be significant.

RESULTS

ERAD of NPC1 Expressed in COS Cells—We reported previously that when FLAG-NPC1 was expressed in COS cells, treatment of the cells with MG132 caused an accumulation of ubiquitylated NPC1. Similar responses were obtained with a loss-of-function mutant P691S, in accordance with the notion that NPC1 underwent ERAD (21). In the current study, we attempted to confirm NPC1 ERAD and tested whether we could reproduce accelerated ERAD of the I1061T mutant, as suggested by other groups (9, 12–14).

MG132 effect on the level of ubiquitylated NPC1 was reproduced in COS cells transiently expressing FLAG-NPC1 together with EGFP (Fig. 1*A*). This drug treatment also caused a clear increase in the steady-state level of FLAG-NPC1. Similar effects were observed with another proteasome inhibitor lactacystin. In contrast, neither lysosomal protease inhibitors chloroquine nor

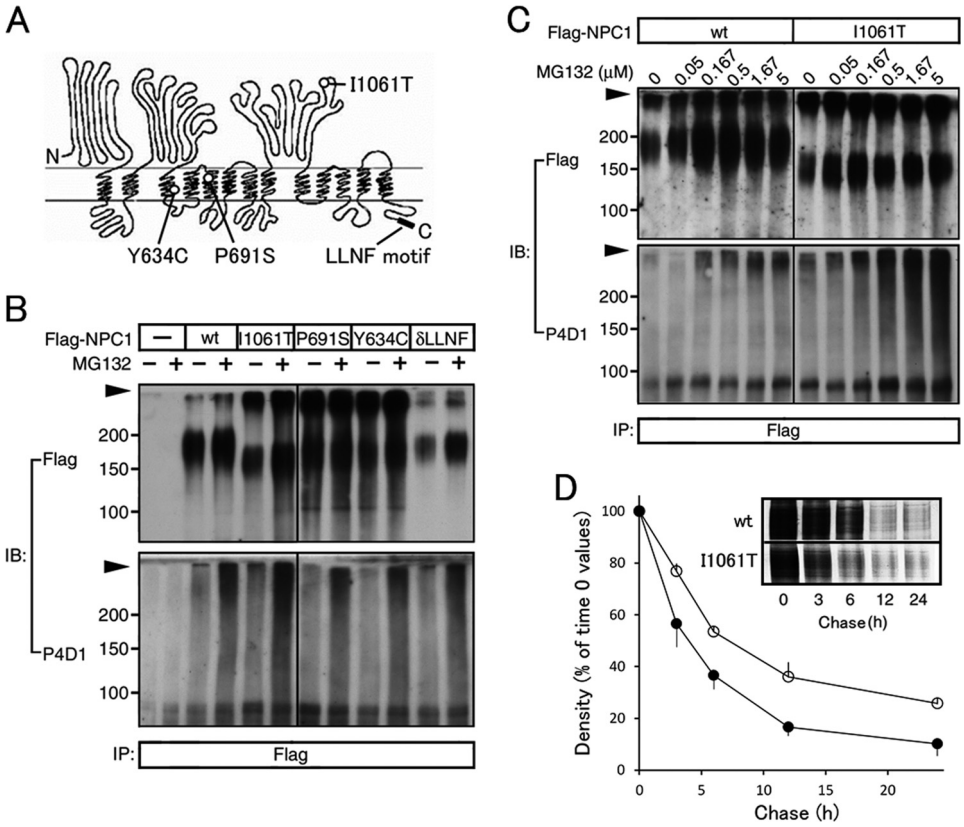

FIGURE 2. **Effects of MG132 on expression and degradation of mutant NPC1.** *A,* schematic representation of NPC1 showing the amino acid substitutions and the LLNF motif. *N* and *C* denote amino and carboxyl terminus, respectively. *B,* steady-state levels of the protein and ubiquitylated form. COS cells were transfected with each FLAG-NPC1 construct. At 48 h post-transfection, cells were cultured for 6 h in the absence or presence of MG132 (5 μM) and anti-FLAG IP products were subjected to IB with anti-FLAG or anti-ubiquitin (P4D1). *C,* dose-dependent effects of MG132. Cells expressing the wild-type or I1061T mutant were cultured for 6 h in the absence or presence of increasing concentrations of MG132 and processed as in *B*. *B* and *C*, shown are the representative results reproduced at least twice. *D,* degradation of the I1061T mutant. Cells were transfected with constructs for the wild-type (*open circles*) or I1061T mutant (*closed circles*) and pulse-labeled and chased as described in the legend to Fig. 1*B*. Each *dot* represents mean ± S.E. of three determinations. $t_{1/2}$ values are given in the text. Representative autoradiographs are shown in the *inset*.

leupeptin affected the steady-state level and caused no accumulation of the ubiquitylated form. Similarly, no effect was observed by addition of NH_4Cl that increases lysosomal pH and inhibits proteolysis in this compartment. As a control, the level of co-expressed EGFP was not affected by MG132 or lactacystin. Accordingly, MG132 more than doubled the half-life time of FLAG-NPC1 as analyzed by pulse-chase labeling (8.6 ± 1.6 and 18.9 ± 1.1 h, mean ± S.E., $n = 3$, in the absence and presence of 5 μM MG132, respectively), whereas chloroquine barely affected the half-life time (9.6 ± 0.8 h in the presence of 0.15 mM chloroquine) (Fig. 1*B*).

Next we examined effects of MG132 on the I1061T mutant, in parallel with other loss-of-function mutants (P691S, Y643C) and an ER-retention mutant δLLNF (Fig. 2*A*). The I1061T mutant protein migrated on electrophoresis faster than the wild-type protein (Fig. 2*B*), most likely because of differential glycosylation (9, 13). MG132 was effective on all of these mutants to induce accumulation of the ubiquitylated form and increase the steady-state levels (Fig. 2*B*). Dose-response analysis revealed that the accumulation of the ubiquitylated I1061T mutant was induced by MG132 more efficiently than that of the wild-type protein (Fig. 2*C*). Pulse-chase labeling (Fig. 2*D*) revealed a markedly shortened half-life time of this mutant protein (9.6 ± 0.5 and 4.2 ± 0.8 h, mean ± S.E., $n = 3$, for the wild-type and I1061T mutant, respectively).

Association of NPC1 with Molecular Chaperones and Its Ubiquitination by CHIP—Molecular chaperones involved in ER quality control can be classified to two categories: one is luminal proteins such as calnexin, and the other is cytosolic proteins such as Hsp40, -70, -90, and Hsc70 (15, 22). Because NPC1 is a multipass membrane protein that has both luminal and cytosolic surfaces, both types of chaperones can be involved in its quality control. To determine molecular chaperones that participate in quality control of NPC1, anti-FLAG IP products from COS cells expressing FLAG-NPC1 were probed with antibodies against each chaperone molecule. As shown in Fig. 3, four kinds of chaperone molecules, Hsp90, Hsp70, Hsc70, and calnexin, were co-precipitated with FLAG-NPC1. In contrast, no Hsp40 was co-precipitated. In addition to its effect on the steady-state level of FLAG-NPC1, MG132 treatment increased the amounts of co-precipitated chaperone molecules. Similar results were reproduced for I1061T and δLLNF mutants (data not shown).

There are a number of E3 ligases that participate in ERAD. One is CHIP that associates with multiple chaperones including Hsp70, Hsc70, and Hsp90 via its TPR domains (23, 24, 25). As expected from co-precipitation of these chaperones, CHIP was also present in the FLAG-NPC1 IP products (Fig. 3). Given this association, we examined whether CHIP could ubiquiti-

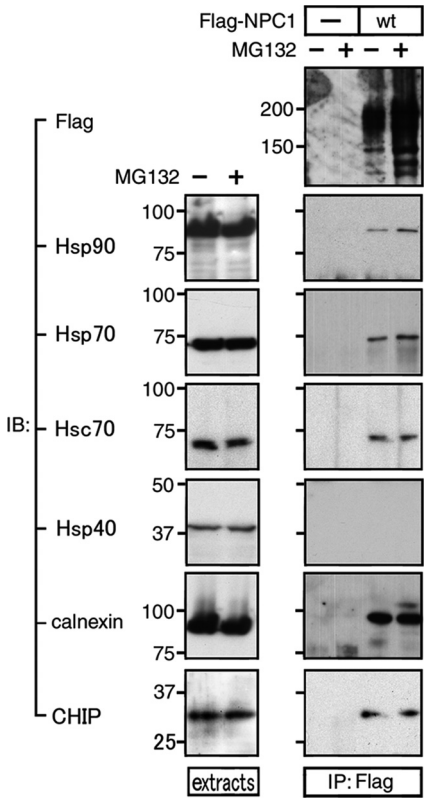

FIGURE 3. **Co-precipitation of chaperone proteins and CHIP with Flag-NPC1.** COS cells were transfected with or without the wild-type FLAG-NPC1 construct. At 48 h post-transfection, cells were cultured for 6 h in the absence or presence of MG132 (5 μM) and 1% Triton X-100 extracts were subjected to anti-FLAG IP followed by IB with the indicated antibodies (*right panel*). The extracts from untransfected cells were also subjected to IB with the indicated antibodies (*left panel*). Shown are representative results reproduced at least twice.

nate NPC1. When FLAG-tagged CHIP was co-expressed with FLAG-NPC1, MG132-induced accumulation of ubiquitylated FLAG-NPC1 was obviously enhanced, whereas this effect was not at all observed with CHIP/δTPR that lacked the TPR domains (Fig. 4*B*). BAG2, originally identified as a component of CHIP-Hsp70 protein complexes, has been shown to disrupt the interaction between CHIP and an E2 ubiquitin-conjugating enzyme and by doing so, eventually suppresses ubiquitination of the substrate (26, 27). Expression of BAG2 suppressed MG132-induced accumulation of ubiquitylated Flag-NPC1 (Fig. 4*C*).

Reciprocal Control of NPC1 Stability by Hsc70 and Hsp70/Hsp90 in HEK Cells—In the case of CHIP substrates such as HERG (human ether-a-go-go-related gene), CFTR (cystic fibrosis transmembrane conductance regulator), and epithelial sodium channels, it has been demonstrated that Hsc70 and Hsp70/Hsp90 exert reciprocal effects on the protein stability, *i.e.* Hsc70 facilitates ubiquitination of the substrate by CHIP leading to its degradation, whereas Hsp70/Hsp90 suppresses ubiquitination leading to its stabilization (18, 28, 29). To see whether NPC1 stability was regulated in a similar manner, we conducted co-expression and RNAi knockdown experiments in HEK cells. This cell line was used because of successful applications of siRNAs against human Hsc70/Hsp70 as well as an HSP90 inhibitor geldanamycin in our previous studies (18, 30).

First we examined effects of co-expressed HSPs on the steady-state level and MG132-induced accumulation of ubiquitylated FLAG-NPC1 and found reciprocal effects of Hsc70 and Hsp70. Hsc70 decreased the steady-state level and exaggerated the accumulation both in MG132-treated and -untreated cells, whereas Hsp70 increased the steady-state level and suppressed MG132-induced accumulation. Hsp90 exhibited marginal effects (Fig. 5*A*).

Next we explored the association of endogenous proteins by co-IP experiments and found that Hsc70, Hsp70, and Hsp90 as well as CHIP were co-precipitated with NPC1 (Fig. 5*B*). Given this association, we tested effects of siRNAs against Hsc70, Hsp70, and CHIP on the levels of endogenous NPC1 and MG132-induced accumulation of its ubiquitylated form and again found reciprocal effects of Hsc70 and Hsp70. siRNA against Hsc70 increased the steady-state level and suppressed accumulation of the ubiquitylated form, whereas siRNA against Hsp70 caused a clear reduction in the steady-state level and exaggerated the accumulation. Like siRNA against Hsc70, siRNA against CHIP increased the steady-state level and suppressed the accumulation of the ubiquitylated form (Fig. 5*C*). We also evaluated effects of geldanamycin as described previously (30) and found that it decreased the level of NPC1 and exaggerated the accumulation of its ubiquitylated form (Fig. 5*D*).

Stabilization of the I1061T Mutant in Human Fibroblasts by HSPs—The above findings indicated accelerated proteasomal degradation of the I1061T mutant and the role of HSPs in its quality control. We then asked whether the endogenous I1061T mutant protein is similarly degraded and, if so, whether it is possible to rescue the mutant protein by increasing the level of HSP. To address these questions, we used primary-cultured fibroblasts from a control subject and NPC patients carrying the I1061T mutation.

First we examined effects of MG132 on the steady-state levels of NPC1 (Fig. 6*A*). As reported elsewhere (7), anti-NPC1 IB gave two bands at 170 and 190kDa in control cell extracts and the level of the mutant NPC1 in the patient's cells was obviously reduced as compared with the level of the wild-type protein in control cells. Although MG132 increased the level of the mutant protein in NPC cells, there appeared to be an appropriate concentration range for this drug to be effective, because it failed to affect the level at concentrations higher than 5 μM. The same drug treatment caused a marginal increase in the level of the wild-type protein in control cells.

Next we examined the effect of Hsp70 overexpression (Fig. 6*B*). Adenovirus-mediated expression of Hsp70 caused a dose-dependent increase in the steady-state level of the mutant NPC1 and as a control, no effect was observed with adeno-LacZ. Given these results, we tested the ability of geranylgeranylacetone (GGA) to increase the level of the mutant NPC1 (Fig. 6*C*). GGA is an anti-ulcer drug that induces expression of HSPs and by doing so, helps maturation of unstable proteins (31, 32). GGA treatment caused a dose-dependent increase in the level of endogenous Hsp70 and Hsp90 and these increases were accompanied by an increase in the protein level of the mutant NPC1. This effect of GGA on the level of NPC1 was

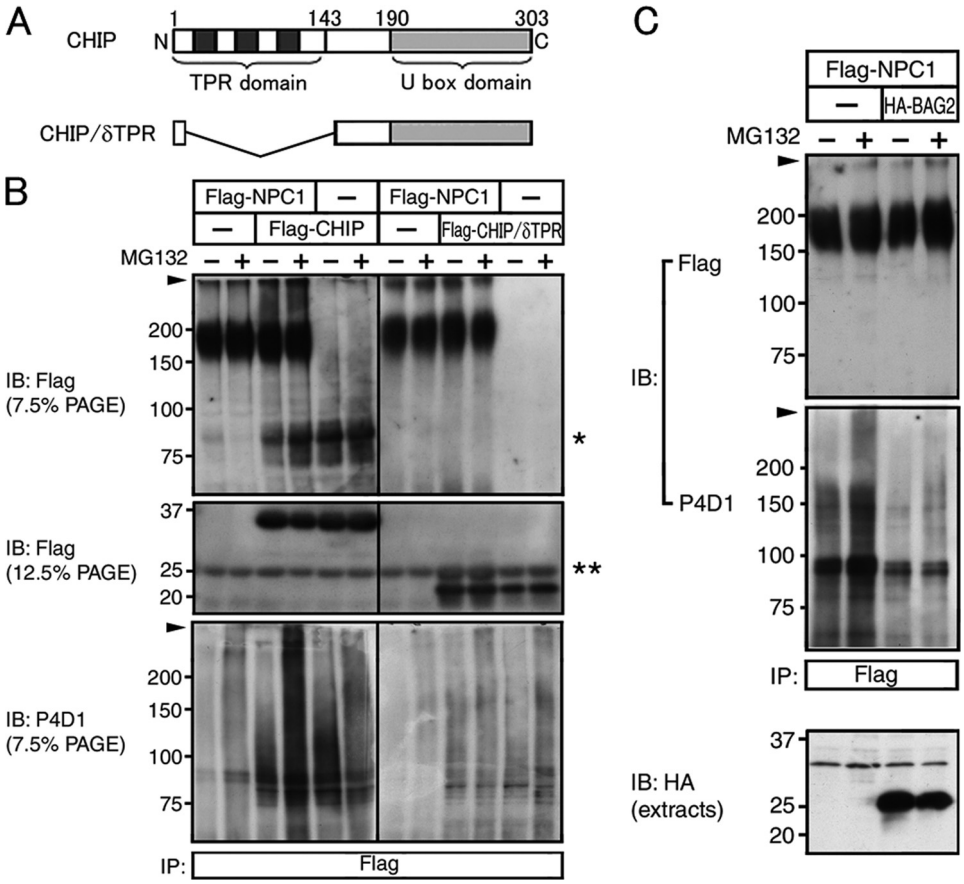

FIGURE 4. **Effects of CHIP or BAG2 on MG132-induced accumulation of ubiquitylated FLAG-NPC1.** *A*, schematic representation of CHIP and its deletion construct δTPR. Each TPR domain is shown in *dark gray*. Amino acid numbers are indicated *above*. *B*, effects of CHIP on the accumulation of ubiquitylated FLAG-NPC1. COS cells were transfected with FLAG-NPC1 alone or together with FLAG-CHIP constructs that encoded the wild-type or δTPR as indicated. At 48 h post-transfection, cells were cultured for 6 h in the absence or presence of MG132 (3 μM) and anti-FLAG IP products were subjected to IB with anti-FLAG or anti-ubiquitin (P4D1). The *single asterisk* indicates the CHIP dimer and the *double asterisk* indicates the immunoglobulin light chain. *C*, effects of BAG2. Cells were transfected with FLAG-NPC1 alone or together with HA-BAG as indicated. After treatment with MG132 at 5 μM for 6 h, cell extracts were subjected to anti-HA IB or anti-FLAG IP. The IP products were probed with anti-FLAG or anti-ubiquitin (P4D1). Shown are representative results reproduced at least twice.

abolished when cells were incubated in the presence of 1 μM geldanamycin (Fig. 6*D*).

We then examined by using subcellular fractionation whether the mutant NPC1 in GGA-treated cells was transported to the late endosome (Fig. 6*E*). When homogenates from NPC cells were fractionated on Opti-prep, the early endosome marker Rab5 was recovered in fractions 2–4, the late endosome marker lamp2 in fractions 3–6, and the ER marker calnexin in fractions 4–12. Hsp70 was recovered in fractions 8–12, both in GGA-untreated and -treated cells, suggesting its association with the ER. As expected, the mutant NPC1 was at detectable levels only in fractions from GGA-treated cells, and was recovered in fractions 3–6, suggesting its localization in the late endosome. These results lead us examine whether GGA could ameliorate the intracellular cholesterol accumulation in these cells (Fig. 6*F*). When NPC cells carrying the I1061T mutation were cultured in the presence of GGA, filipin staining revealed a clear reduction of cholesterol accumulation. This effect was not observed in cells carrying sterol-sensing domain mutations F705S/S813X.

Identification of Ubiquitin-conjugation Sites of NPC1—We used MALDI-TOF mass spectrometry to identify lysine residues of NPC1 that potentially accept ubiquitin. The strategy depends on the fact that trypsin digestion of ubiquitin-conjugated proteins produces diglycine-branched peptides in which the C-terminal Gly-Gly fragment of ubiquitin is attached to the ε-amino group of a modified lysine residue within the peptide (33). In practice, CHO/FLAG-NPC1 knock-in cells were incubated in the absence or presence of 5 μM MG132 for 6 h and FLAG-NPC1 was recovered from cell extracts by IP and was separated on PAGE. FLAG-NPC1 in excised gel plugs was digested with trypsin and the peptide mixture was analyzed using a MALDI-TOF mass spectrometer. This digestion yielded 194 and 146 peptides derived from FLAG-NPC1 in MG132-treated and -untreated samples, respectively. Comparison between the measured mass and the theoretical mass of each peptide showed that 15 peptides in the MG132-treated sample were potentially modified with a Gly-Gly fragment (Table 1). Of these 15 peptides, 9 were also predicted to be modified with a Gly-Gly fragment in MG132-untreated samples. Of the 6 peptides that were predicted to be specifically modified in the MG132-treated sample, 3 peptides corresponded to the amino acid sequences that contained a lysine residue on the cytosolic loops of NPC1. The sequences of the 3 peptides were DKGEASCCDPVSAAFEGCLR (amino acids 317–336), RQEKNR (amino acids 789–794), and AFTVSMKGSRVER (amino acids 1174–1186). The other 3 peptides corresponded to

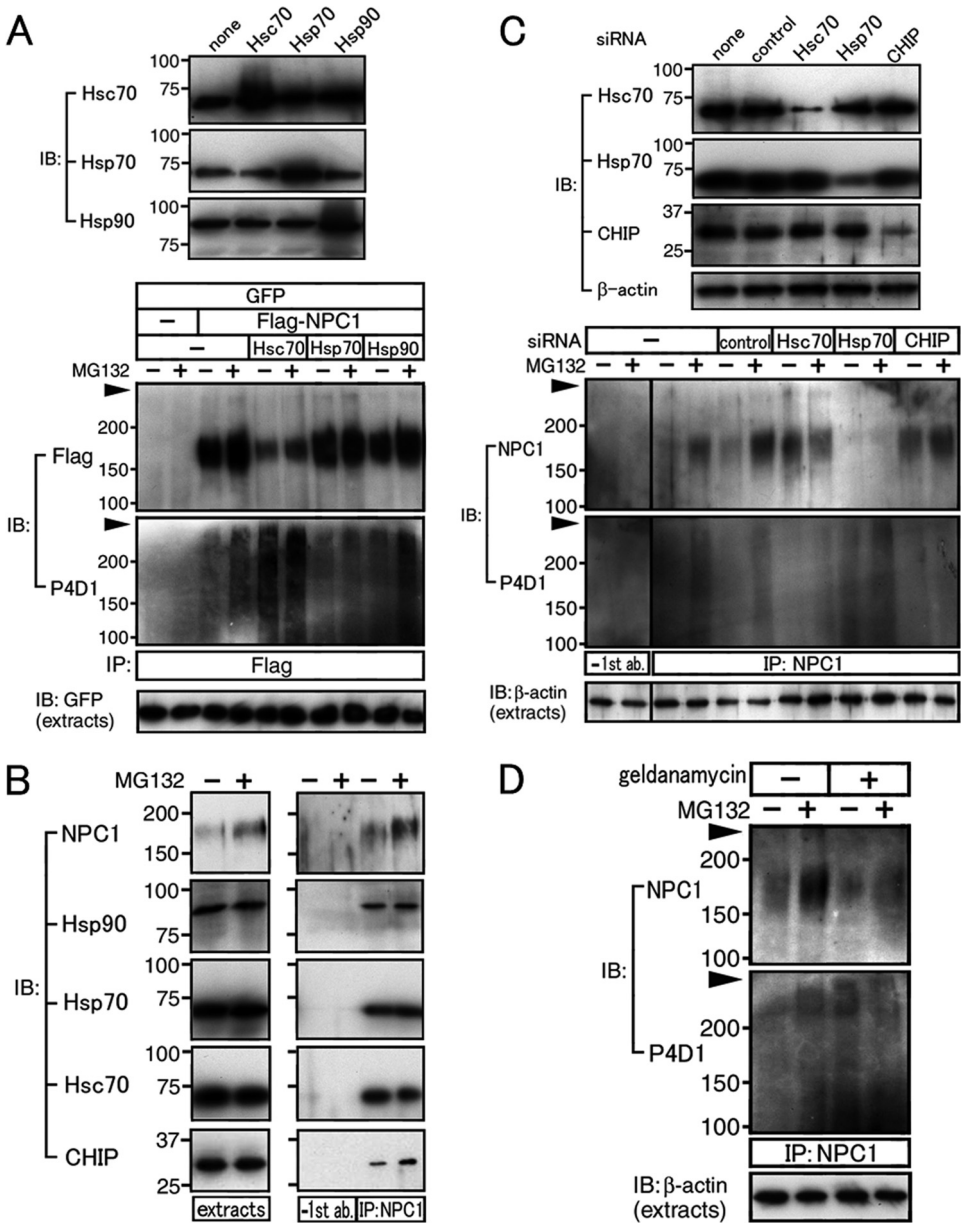

FIGURE 5. **Regulation of NPC1 stability by HSPs/CHIP in HEK cells.** *A*, effects of co-expression of HSPs on the expression level of FLAG-NPC1. *Upper panel*, cells were transfected with each HSP construct and at 48 h post-transfection, 1% Triton X-100 extracts were harvested and subjected to IB with the indicated antibodies. *Lower panel*, cells were transfected with FLAG-NPC1 alone or together with each HSP construct. At 48 h post-transfection, they were cultured for 6 h in the absence or presence of MG132 (5 μM) and anti-FLAG IP products were subjected to IB with anti-FLAG or anti-ubiquitin (P4D1). *B*, co-precipitation of chaperone proteins with NPC1. Cells were cultured for 6 h in the absence or presence of MG132 (5 μM) and 1% Triton X-100 extracts were subjected to anti-NPC1 IP. The extracts and IP products were subjected to IB. *C*, effects of RNAi knockdown of HSP/CHIP. *Upper panel*, cells were transfected with each siRNA and at 48 h post-transfection, 1% Triton X-100 extracts were harvested and subjected to IB. *Lower panel*, cells were transfected with each siRNA. At 48 h post-transfection, cells were cultured for 6 h in the absence or presence of MG132 (5 μM) and anti-NPC1 IP products were subjected to IB. −*1st ab*, IP was conducted without the primary antibody. *D*, effects of geldanamycin. Cells were incubated in the absence or presence of geldanamycin (1 μM) overnight and further incubated in the absence or presence of MG132 (5 μM) for 6 h. 1% Triton X-100 extracts were subjected to anti-NPC1 IP followed by IB. Shown are the representative results reproduced at least twice.

the amino acid sequences on the luminal loops of NPC1, which are unlikely to be accessible to ubiquitin ligases. Thus, this analysis identified the three lysine residues at amino acids 318, 792, and 1180 as potential ubiquitin-conjugation sites of NPC1.

To confirm conjugation of ubiquitin to these residues and to assess their role in NPC1 degradation, we generated a series of mutants with single (S1, S2, S3), double (D1, D2, D3), or triple (T1) lysine to alanine substitutions as listed in Fig. 7*A*. When expressed in COS cells, the steady-state levels of these mutants were obviously higher than that of the wild-type protein and appeared to be in an order of the wild-type < S series < D series < T1 (Fig. 7*B*). Densitometry showed that expression levels of the three S series mutants were within a similar range and the same was the case for D series mutants (Fig. 7*C*). Pulse-chase labeling (Fig. 7*D*) revealed a markedly prolonged half-life time of T1 (8.0 ± 1.3 and 20 ± 0.6 h, mean ± S.E., $n = 3$, for the wild-type and T1, respectively). We then examined effects of MG132 (Fig. 7*E*). Like in the case of wild-type, MG132 treat-

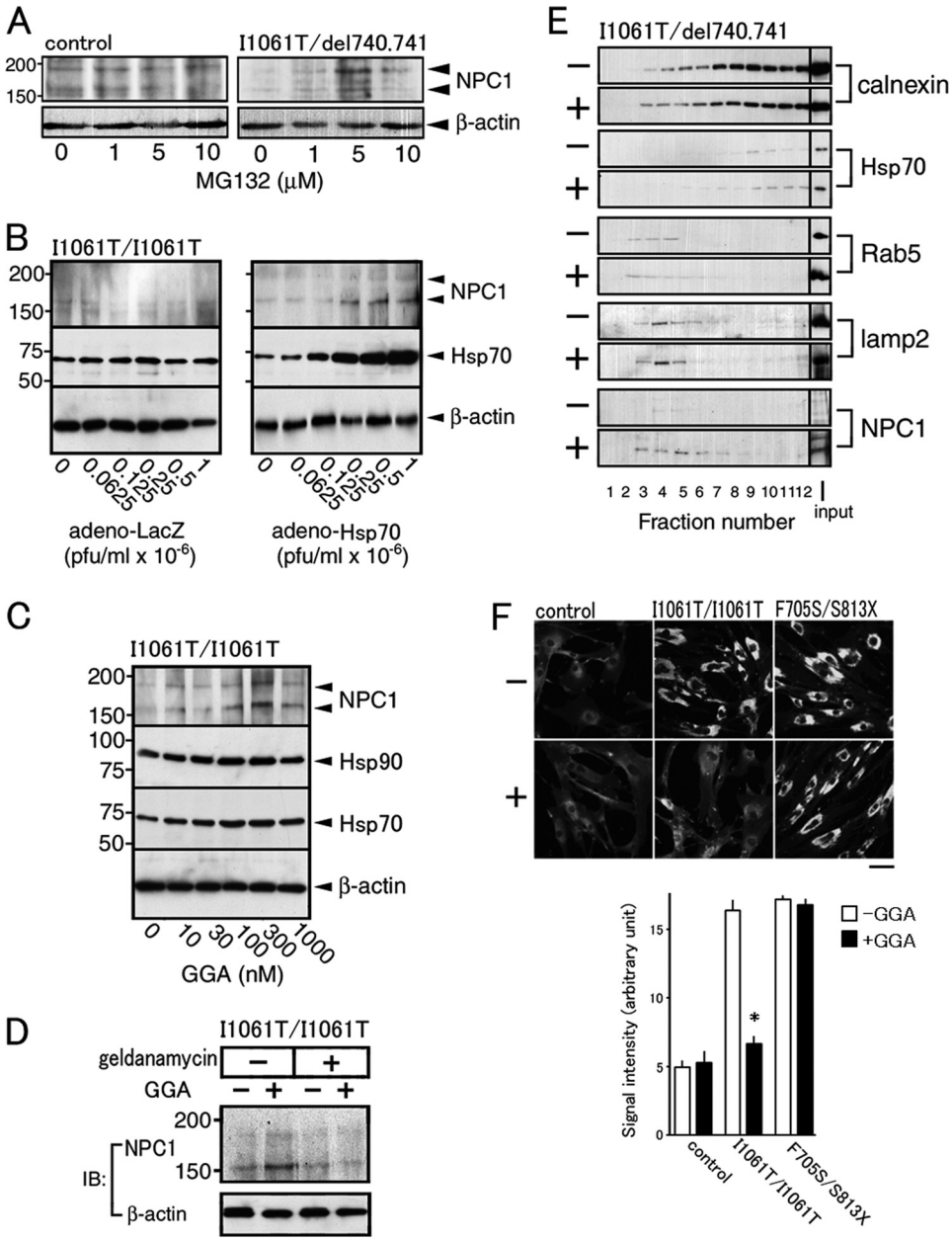

FIGURE 6. **Stabilization of the I1061T mutant by HSPs in human fibroblasts.** *A,* effects of MG132 on the protein level of NPC1. Cells were cultured in the absence or presence of increasing concentrations of MG132 for 6 h and 1% Triton X-100 extracts were subjected to IB with anti-NPC1 or anti-β-actin. Shown are the representative blots using cells from a control subject or a patient heterozygous for I1061T. Similar results were reproduced using cells from a patient homozygous for I1061T. *B*, effects of adenovirus-mediated expression of Hsp70. Cells were exposed to adenovirus carrying LacZ or Hsp70 and at 48 h post-transfection, 1% Triton X-100 extracts were subjected to IBs. *C*, effects of GGA. Cells were cultured in the absence or presence of increasing concentrations of GGA for 24 h and cell extracts were subjected to IB. *D*, effects of geldanamycin. Cells were incubated for 24 h in the absence or presence of geldanamycin (1 μM) or GGA (0.3 μM) as indicated and cell extracts were subjected to IB. *E*, subcellular distribution of NPC1. After treatment with (+) or without (−) GGA (0.3 μM for 24 h), cell homogenates were fractionated on an Opti-prep gradient. The fractions, together with the homogenates applied (*input*), were analyzed by IB. Shown are representative blots using cells from a patient heterozygous for I1061T. Similar results were reproduced using cells from a patient homozygous for I1061T. All in *A–E*, shown are the representative results, which were reproduced at least twice. *F*, effects of GGA on intracellular cholesterol accumulation. After treatment with or without GGA (0.3 μM for 48 h), cells were fixed and stained with filipin. Shown are representative images obtained with a fluorescent microscope and results of densitometry. Each *bar* represents mean ± S.E. of three determinations. Signals from more than 10 cells were evaluated in each experiment. *, $p < 0.01$, significantly different from the values in untreated cells. *Bar*, 50 μm.

ment at 5 μM for 6 h caused an apparent increase in the steady-state levels of S series mutants. This effect was obscured in D series mutants and was absent in T1. MG132-induced accumulation of the ubiquitylated form was reduced in S series mutants, as compared with that of the wild-type, further reduced in D series mutants, and was undetectable in T1. These findings are consistent with conjugation of ubiquitin to the three lysine residues and suggested their critical role in the regulation of NPC1 ERAD.

Finally, we asked whether the T1 mutant was functional and if so, whether elimination of the three lysine residues could rescue the I1061T mutant from ERAD. To address the first question, T1 was transiently expressed in CHO/NPC1(−) cells and by staining with filipin, its function was compared with that

TABLE 1

FLAG-NPC1-derived peptides predicted to be modified with a Gly-Gly fragment(s)

+ and − denote samples from MG132-treated and -untreated cells, respectively. Amino acid residues derived from the FLAG tag (shown in lowercase letters) were excluded from the amino acid numbering.

No.	Start	End	Peptide sequence	Modifications	Detected in	Position
1	789	794	RQEKNR	1 Gly-Gly	+ only	Cytosolic, Lys-792
2	37	42	DKRYNC	1 Gly-Gly	+, −	
3	1174	1186	AFTVSMKGSRVER	1 Gly-Gly	+ only	Cytosolic, Lys-1180
4	307	318	dkSNIAFSVNASDK	1 Gly-Gly	+−	
5	985	997	EGKQRPQGGDFMR	1 Gly-Gly	+ only	Luminal
6	295	306	KRYFVSEYTPId	1 Gly-Gly	+−	
7	164	181	EAPSSNDKALGLLCGKDA	1 Gly-Gly	+−	
8	391	404	EKEYFDQHFGPFFR	1 Gly-Gly	+−	
9	162	181	DVEAPSSNDKALGLLCGKDA	1 Gly-Gly	+−	
10	580	595	AQAWEKEFINFVKNYK	2 Gly-Gly	+−	
11	789	805	RQEKNRLDIFCCVRGAE	1 Gly-Gly	+−	
12	295	305	KRYFVSEYTPIddyd	2 Gly-Gly	+−	
13	317	336	DKGEASCCDPVSAAFEGCLR	1 Gly-Gly	+ only	Cytosolic, Lys-318
14	40	60	YNCEYSGPPKPLPKDGYDLVQ	2 Gly-Gly	+ only	Luminal
15	868	893	DDSYMVDYFKSISQYLHAGPPVYFVL	1 Gly-Gly	+ only	Luminal

of the wild-type. To address the second question, we engineered a construct that carried both the triple substitutions and I1061T (I1061T/T1) and its function was compared with that of the I1061T. Transient expression in CHO/NPC1(−) cells showed that the protein level of the I1061T/T1 was obviously higher than that of the I1061T (Fig. 8*A*). Like the wild-type, expression of T1 abolished the intracellular cholesterol accumulation almost completely, suggesting that elimination of the three lysine residues did not interfere with NPC1 function (Fig. 8*B*). The effects of the I1061T mutant were variable in individual cells that expressed this mutant: in some cells it caused only a marginal effect, whereas in others it partially reduced the accumulation. Quantification of filipin signals from multiple cells showed that on average, the cholesterol accumulation was reduced by ~30% in cells expressing the I1061T. The same quantification showed that expression of the I1061T/T1 caused almost complete clearance of the accumulation (Fig. 8*C*).

DISCUSSION

Using human skin fibroblasts, several laboratories have presented evidence for NPC1 ERAD and accelerated degradation of the I1061T mutant (9, 12–14). In the current study, we confirmed NPC1 ERAD using transient expression in COS cells. Consistent with proteasomal degradation of NPC1, the proteasome inhibitor MG132 increased the steady-state level of the expressed protein, caused an accumulation of its ubiquitylated form, and prolonged its life span (Fig. 1). The ubiquitination, at least partially, takes place in the ER, because of the MG132-induced accumulation of the ubiquitylated form of an ER-retention mutant δLLNF (Fig. 2). Because mature NPC1 primarily resides in the late endosome, it is most likely that this modification and degradation occurs during biosynthesis of this protein. The negative effects of lysosomal protease inhibitors suggest that NPC1 is minimally degraded in the lysosome and it remains to be clarified how mature NPC1 is degraded. We could also reproduce accelerated ERAD of the I1061T mutant in our expression experiments, as indicated by its reduced life span and an exaggerated accumulation of its ubiquitylated form in the presence of MG132 (Fig. 2).

As for the molecular chaperones involved in quality control of NPC1, overexpression of calnexin was found to increase the protein level of the I1061T mutant in patient-derived fibroblasts (12). Here we presented evidence for involvement of multiple HSPs including Hsc70, Hsp70, and Hsp90 in NPC1 quality control (Fig. 3). Accordingly, overexpression of CHIP enhanced MG132-induced accumulation of its ubiquitylated form (Fig. 4*B*). Together with suppression of the accumulation by BAG2 (Fig. 4*C*) and CHIP siRNA (Fig. 5*C*), these results suggested that CHIP is one of the E3 ligases responsible for NPC1 ubiquitination. Transient expression and siRNA knockdown experiments in HEK cells (Fig. 5) suggested that as in the case of other CHIP/HSP clients, NPC1 stability was regulated by Hsc70 and Hsp70/Hsp90 in a reciprocal manner, *i.e.* Hsc70 facilitates its ubiquitination leading to degradation, whereas Hsp70/Hsp90 exerts the opposite effect. Co-expression experiments showed a marginal effect of Hsp90 on the level of FLAG-NPC1 and MG132-induced accumulation of its ubiquitylated form (Fig. 5*A*). However, geldanamycin caused a significant reduction in the level of endogenous NPC1 and exaggerated its ubiquitination (Fig. 5*D*), suggesting that Hsp90 was also able to stabilize NPC1.

NPC1 contains a sterol-sensing domain (4). In the case of HMG-CoA reductase that also contains this domain, it is well established that gp78, a membrane-anchored E3 ligase, associates with Insig-1 and couples sterol-regulated ubiquitination to proteasomal degradation (34). We reported previously that in COS cells, MG132-induced accumulation of ubiquitylated FLAG-NPC1 was not affected by the cellular cholesterol level (21). We found in the current study that in COS cells, co-expressed FLAG-gp78 failed to enhance the MG132 effect on ubiquitination of FLAG-NPC1 and that in HEK cells, endogenous Insig-1 was not co-precipitated with NPC1 (data not shown). These lines of negative data argue against the role of gp78 in NPC1 ERAD and also suggest that unlike HMG-CoA reductase, NPC1 degradation is not regulated by the cellular cholesterol level.

Because the cooperative activity of HSPs and CHIP is involved in the quality control of multiple client proteins (24), it is not surprising that NPC1 is one of those clients. Importantly, however, we could increase the protein level of the I1061T mutant in patient-derived fibroblasts by overexpression of Hsp70, and this effect was mimicked by GGA, which has an

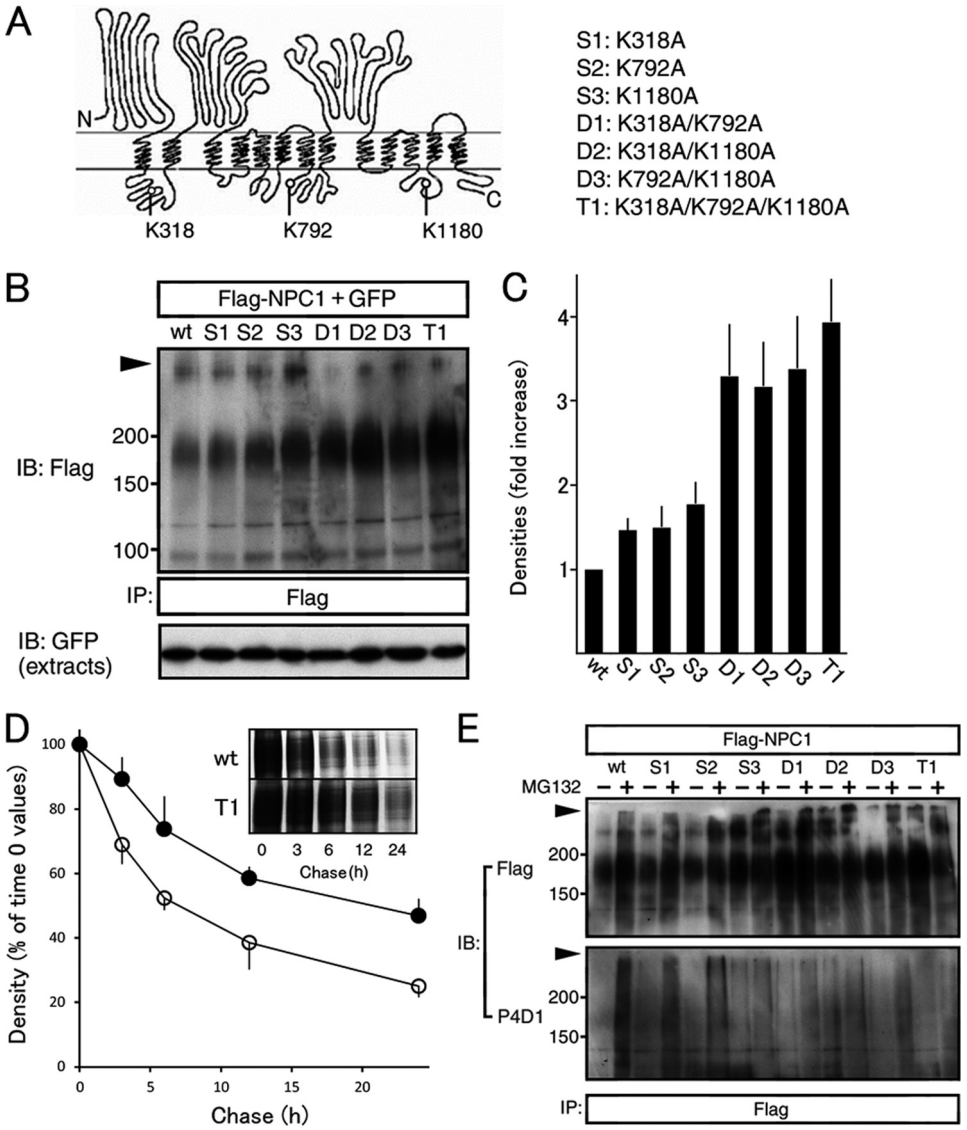

FIGURE 7. **Characterization of NPC1 mutants that lack potential ubiquitin-conjugation sites.** *A,* schematic representation of NPC1 showing the three lysine residues predicted by MALDI-TOF mass spectrometry to accept ubiquitin. Single, double, and triple substitutions were introduced to FLAG-NPC1 as listed. *B*, steady-state levels of the mutants expressed in COS cells. Cells were transfected with each construct together with pEGFP. 1% Triton X-100 extracts were subjected to anti-GFP IB or anti-FLAG IP followed by anti-FLAG IB. *C,* densitometry of the data shown in *B*. Band densities were quantified and expressed as relative to the values of the wild-type. Each *bar* represents mean ± S.E. of three determinations. *D*, degradation of the T1 mutant. Cells were transfected with constructs for the wild-type (*open circles*) or T1 mutant (*closed circles*) and they were pulse-labeled and chased as described in the legend to Fig. 1*B*. Each *dot* represents mean ± S.E. of three determinations. $t_{1/2}$ values are given in the text. Representative autoradiographs are shown in the *inset*. *E,* effects of MG132. Transfected cells were treated with or without MG132 at 5 μM for 6 h. Anti-FLAG IP products were probed with the indicated antibodies. Shown are representative results reproduced at least twice.

activity to induce expression of HSPs (Fig. 6). Geldanamycin suppressed the GGA effect (Fig. 6*D*) suggesting that the activity of Hsp90 was indispensable for GGA to be effective. In GGA-treated cells, the I1061T protein was localized in the endosomal fractions and ameliorated the cholesterol accumulation (Fig. 6, *E* and *F*), consistent with the notion that the I1061T mutant retains NPC1 function (9). GGA can be orally administrated and reach the brain, and it has been shown to alleviate neurodegeneration in an animal model of spinal and bulbar muscular atrophy (31). To pursuit its potential as a therapy, its effects in NPC animal models should be the subject in future studies.

With respect to pharmacological rescue of NPC1 mutants, two recent studies demonstrated the capacity of histone deacetylase inhibitors to increase expression of mutant NPC1 proteins and to correct cholesterol storage defects in human NPC cells (35, 36). Histone deacetylase inhibitors appear to have pleiotropic effects both at transcriptional and post-transcriptional levels. ERAD is one of the processes modulated by these agents as evidenced by enhanced acetylation of Hsp90 in cells treated with them (37) and increased expression of BAG2 in cells treated with siRNA against histone deacetylase (38).

MALDI-TOF mass spectrometry predicted conjugation of ubiquitin to three lysine residues at amino acids 318, 792, and 1180 and experiments using a series of substitution mutants provided two lines of evidence for modification of these residues (Fig. 7). First, the steady-state levels of the substitution mutants were inversely related to the number of potential ubiquitination sites, in an order of the wild-type < S series < D

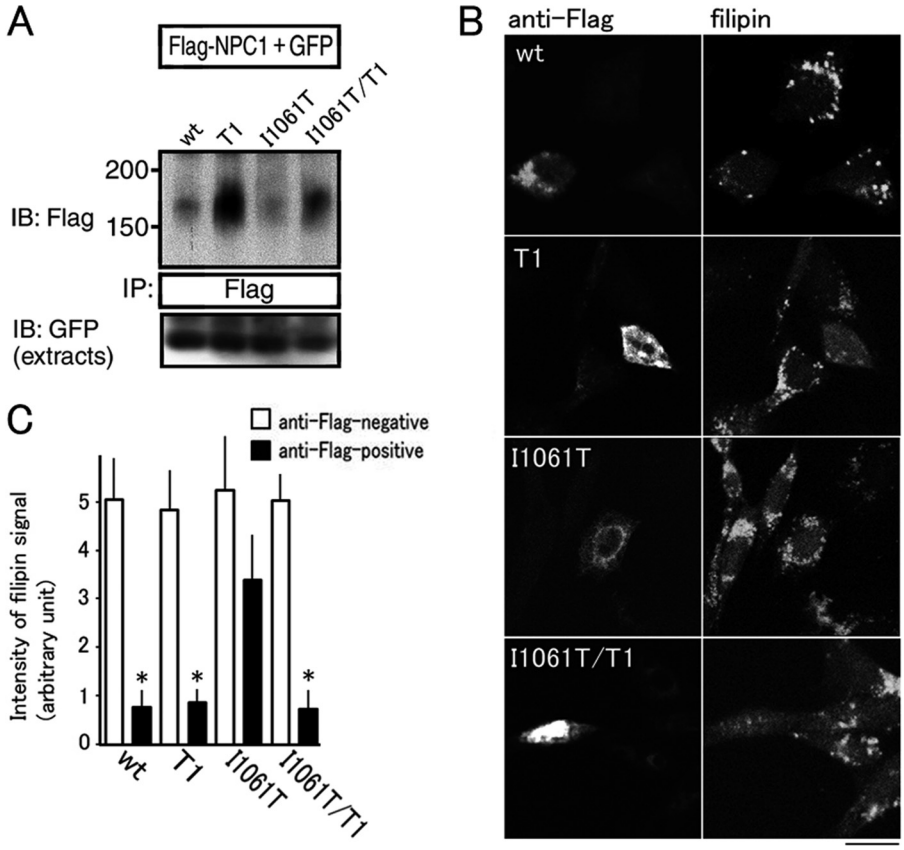

FIGURE 8. **Function of the triple substitution mutant to rescue intracellular cholesterol accumulation.** *A,* steady-state levels of the mutants expressed in CHO/NPC1(−) cells. Cells were transfected with each construct together with pEGFP. 1% Triton X-100 extracts were subjected to anti-GFP IB or anti-FLAG IP followed by anti-FLAG IB. Shown are the representative blots reproduced at least twice. *B,* intracellular cholesterol accumulation. CHO/NPC1(−) cells were transfected with each construct and at 48 h post-transfection, subjected to anti-FLAG immunostaining followed by filipin staining. Shown are representative images obtained with a confocal microscope. *Bar*, 25 μm. *C*, densitometry of the data shown in *B*. Quantification of filipin signals was performed as described in the legend to Fig. 6*F*. Each *bar* represents mean ± S.E. of three determinations. Signals from more than 10 cells that were either negatively or positively stained with anti-FLAG were evaluated in each experiment. *, $p < 0.01$, significantly different from the values in anti-FLAG negative cells.

series < T1. Second, the levels of MG132-induced accumulation of the ubiquitylated form appeared to depend on the number of potential ubiquitination sites, in an order of the wild-type > S series > D series > T1. These findings were consistent with conjugation of ubiquitin to these three lysine residues. Furthermore, they suggested that conjugation to individual lysine residues operates independently from each other and is functionally equivalent as a tag for protein degradation.

Biosynthesis of NPC1 appeared to be intrinsically an inefficient process, because it is estimated that more than two-thirds of the wild-type protein is degraded by ERAD, based on the observation that the steady-state level of expressed T1 was more than three times higher than that of the wild-type protein. This is consistent with the report by Gelsthorpe *et al.* (9) in which it was estimated that ~50% of NPC1 in human fibroblasts was retained in the ER and targeted for degradation. We also showed that the triple substitutions did not interfere with NPC1 function but rather restored function of the I1061T mutant (Fig. 8). These results provided another line of evidence for accelerated degradation of the I1061T mutant. They are also consistent with the fact that none of the three lysine residues are included in the disease-causing mutations so far reported (NPC gene variation database).

In summary, we confirmed NPC1 ERAD, provided evidence for the role of HSPs in its quality control, and revealed the role of three lysine residues as ubiquitin-conjugation sites. These lines of information will be of value in future attempts to develop a pharmacological chaperone therapy that aims at stabilization of unstable, mutant NPC1 proteins.

REFERENCES

1. Patterson, M. C., Vanier, M. T., Suzuki, K., Morris, J. A., Carstea, E. D., Neufeld, E. B., Blanchette-Mackie, E. J., and Pentchev, P. G. (2001) Niemann-Pick disease type C: a lipid trafficking disorder. in *The metabolic and molecular bases of inherited disease* (Scriver, C. R., Beaudet, A. L., Sly, W. S., Valle, D., Childs, B., Kinzler, K. W., and Vogelstein, B., eds) pp. 3611–3634, McGraw Hill, New York
2. Carstea, E. D., Morris, J. A., Coleman, K. G., Loftus, S. K., Zhang, D., Cummings, C., Gu, J., Rosenfeld, M. A., Pavan, W. J., Krizman, D. B., Nagle, J., Polymeropoulos, M. H., Sturley, S. L., Ioannou, Y. A., Higgins, M. E., Comly, M., Cooney, A., Brown, A., Kaneski, C. R., Blanchette-Mackie, E. J., Dwyer, N. K., Neufeld, E. B., Chang, T. Y., Liscum, L., Strauss, J. F., 3rd, Ohno, K., Zeigler, M., Carmi, R., Sokol, J., Markie, D., O'Neill, R. R., van Diggelen, O. P., Elleder, M., Patterson, M. C., Brady, R. O., Vanier, M. T., Pentchev, P. G., and Tagle, D. A. (1997) Niemann-Pick C1 disease gene: homology to mediators of cholesterol homeostasis. *Science* **277,** 228–231
3. Naureckiene, S., Sleat, D. E., Lackland, H., Fensom, A., Vanier, M. T., Wattiaux, R., Jadot, M., and Lobel, P. (2000) Identification of HE1 as the second gene of Niemann-Pick C disease. *Science* **290,** 2298–2301
4. Higgins, M. E., Davies, J. P., Chen, F. W., and Ioannou, Y. A. (1999) Niemann-Pick C1 is a late endosome-resident protein that transiently associates with lysosomes and the trans-Golgi network. *Mol. Genet. Metab.* **68,** 1–13
5. Vanier, M. T., and Millat, G. (2004) Structure and function of the NPC2

protein. *Biochim. Biophys. Acta* **1685,** 14–21
6. Sévin, M., Lesca, G., Baumann, N., Millat, G., Lyon-Caen, O., Vanier, M. T., and Sedel, F. (2007) The adult form of Niemann-Pick disease type C. *Brain* **130,** 120–133
7. Yamamoto, T., Ninomiya, H., Matsumoto, M., Ohta, Y., Nanba, E., Tsutsumi, Y., Yamakawa, K., Millat, G., Vanier, M. T., Pentchev, P. G., and Ohno, K. (2000) Genotype-phenotype relationship of Niemann-Pick disease type C: a possible correlation between clinical onset and levels of NPC1 protein in isolated skin fibroblasts. *J. Med. Genet.* **37,** 707–712
8. Millat, G., Marçais, C., Tomasetto, C., Chikh, K., Fensom, A. H., Harzer, K., Wenger, D. A., Ohno, K., and Vanier, M. T. (2001) Niemann-Pick C1 disease: correlations between NPC1 mutations, levels of NPC1 protein, and phenotypes emphasize the functional significance of the putative sterol-sensing domain and of the cysteine-rich luminal loop. *Am. J. Hum. Genet.* **68,** 1373–1385
9. Gelsthorpe, M. E., Baumann, N., Millard, E., Gale, S. E., Langmade, S. J., Schaffer, J. E., and Ory, D. S. (2008) Niemann-Pick type C1 I1061T mutant encodes a functional protein that is selected for endoplasmic reticulum-associated degradation due to protein misfolding. *J. Biol. Chem.* **283,** 8229–8236
10. Sugimoto, Y., Ninomiya, H., Ohsaki, Y., Higaki, K., Davies, J. P., Ioannou, Y. A., and Ohno, K. (2001) Accumulation of cholera toxin and GM1 ganglioside in the early endosome of Niemann-Pick C1-deficient cells. *Proc. Natl. Acad. Sci. U.S.A.* **98,** 12391–12396
11. Yamamoto, T., Feng, J. H., Higaki, K., Taniguchi, M., Nanba, E., Ninomiya, H., and Ohno, K. (2004) Increased NPC1 mRNA in skin fibroblasts from Niemann-Pick disease type C patients. *Brain Dev.* **26,** 245–250
12. Yu, T., Chung, C., Shen, D., Xu, H., and Lieberman, A. P. (2012) Ryanodine receptor antagonists adapt NPC1 proteostasis to ameliorate lipid storage in Niemann-Pick type C disease fibroblasts. *Hum. Mol. Genet.* **21,** 3205–3214
13. Zampieri, S., Bembi, B., Rosso, N., Filocamo, M., and Dardis, A. (2012) Treatment of human fibroblasts carrying NPC1 missense mutations with MG132 leads to an improvement of intracellular cholesterol trafficking. *JIMD Rep.* **2,** 59–69
14. Ohgane, K., Karaki, F., Dodo, K., and Hashimoto, Y. (2013) Discovery of oxysterol-derived pharmacological chaperones for NPC1: implication for the existence of second sterol-binding site. *Chem. Biol.* **20,** 391–402
15. Brodsky, J. L. (2012) Cleaning up: ER-associated degradation to the rescue. *Cell* **151,** 1163–1167
16. Needham, P. G., and Brodsky, J. L. (2013) How early studies on secreted and membrane protein quality control gave rise to the ER associated degradation (ERAD) pathway: the early history of ERAD. *Biochim. Biophys. Acta* **1833,** 2447–2457
17. Davies, J. P., and Ioannou, Y. A. (2000) Topological analysis of Niemann-Pick C1 protein reveals that the membrane orientation of the putative sterol-sensing domain is identical to those of 3-hydroxy-3-methylglutaryl-CoA reductase and sterol regulatory element binding protein cleavage-activating protein. *J. Biol. Chem.* **275,** 24367–24374
18. Li, P., Ninomiya, H., Kurata, Y., Kato, M., Miake, J., Yamamoto, Y., Igawa, O., Nakai, A., Higaki, K., Toyoda, F., Wu, J., Horie, M., Matsuura, H., Yoshida, A., Shirayoshi, Y., Hiraoka, M., and Hisatome, I. (2011) Reciprocal control of hERG stability by Hsp70 and Hsc70 with implication for restoration of LQT2 mutant stability. *Circ. Res.* **108,** 458–468
19. Fujimoto, M., Takaki, E., Hayashi, T., Kitaura, Y., Tanaka, Y., Inouye, S., and Nakai, A. (2005) Active HSF1 significantly suppresses polyglutamine aggregate formation in cellular and mouse models. *J. Biol. Chem.* **280,** 34908–34916
20. Lin, H., Sugimoto, Y., Ohsaki, Y., Ninomiya, H., Oka, A., Taniguchi, M., Ida, H., Eto, Y., Ogawa, S., Matsuzaki, Y., Sawa, M., Inoue, T., Higaki, K., Nanba, E., Ohno, K., and Suzuki, Y. (2004) *N*-Octyl-β-valienamine up-regulates activity of F213I mutant β-glucosidase in cultured cells: a potential chemical chaperone therapy for Gaucher disease. *Biochim. Biophys. Acta* **1689,** 219–228
21. Ohsaki, Y., Sugimoto, Y., Suzuki, M., Hosokawa, H., Yoshimori, T., Davies, J. P., Ioannou, Y. A., Vanier, M. T., Ohno, K., and Ninomiya, H. (2006) Cholesterol depletion facilitates ubiquitination of NPC1 and its association with SKD1/Vps4. *J. Cell Sci.* **119,** 2643–2653
22. McClellan, A. J., Tam, S., Kaganovich, D., and Frydman, J. (2005) Protein quality control: chaperones culling corrupt conformations. *Nat. Cell Biol.* **7,** 736–741
23. Murata, S., Minami, Y., Minami, M., Chiba, T., and Tanaka, K. (2001) CHIP is a chaperone-dependent E3 ligase that ubiquitylates unfolded protein. *EMBO Rep.* **2,** 1133–1138
24. Meusser, B., Hirsch, C., Jarosch, E., and Sommer, T. (2005) ERAD: the long road to destruction. *Nat. Cell Biol.* **7,** 766–772
25. Matsumura, Y., Sakai, J., and Skach, W. R. (2013) Endoplasmic reticulum protein quality control is determined by cooperative interactions between Hsp/c70 and the CHIP E3 ligase. *J. Biol. Chem.* **288,** 31069–31079
26. Dai, Q., Qian, S. B., Li, H. H., McDonough, H., Borchers, C., Huang, D., Takayama, S., Younger, J. M., Ren, H. Y., Cyr, D. M., and Patterson, C. (2005) Regulation of the cytoplasmic quality control protein degradation pathway by BAG2. *J. Biol. Chem.* **280,** 38673–38681
27. Arndt, V., Daniel, C., Nastainczyk, W., Alberti, S., and Höhfeld, J. (2005) BAG-2 acts as an inhibitor of the chaperone-associated ubiquitin ligase CHIP. *Mol. Biol. Cell* **16,** 5891–5900
28. Meacham, G. C., Patterson, C., Zhang, W., Younger, J. M., and Cyr, D. M. (2001) The Hsc70 co-chaperone CHIP targets immature CFTR for proteasomal degradation. *Nat. Cell Biol.* **3,** 100–105
29. Goldfarb, S. B., Kashlan, O. B., Watkins, J. N., Suaud, L., Yan, W., Kleyman, T. R., and Rubenstein, R. C. (2006) Differential effects of Hsc70 and Hsp70 on the intracellular trafficking and functional expression of epithelial sodium channels. *Proc. Natl. Acad. Sci. U.S.A.* **103,** 5817–5822
30. Iwai, C., Li, P., Kurata, Y., Hoshikawa, Y., Morikawa, K., Maharani, N., Higaki, K., Sasano, T., Notsu, T., Ishido, Y., Miake, J., Yamamoto, Y., Shirayoshi, Y., Ninomiya, H., Nakai, A., Murata, S., Yoshida, A., Yamamoto, K., Hiraoka, M., and Hisatome, I. (2013) Hsp90 prevents interaction between CHIP and HERG proteins to facilitate maturation of wild-type and mutant HERG proteins. *Cardiovasc. Res.* **100,** 520–528
31. Katsuno, M., Sang, C., Adachi, H., Minamiyama, M., Waza, M., Tanaka, F., Doyu, M., and Sobue, G. (2005) Pharmacological induction of heat-shock proteins alleviates polyglutamine-mediated motor neuron disease. *Proc. Natl. Acad. Sci. U.S.A.* **102,** 16801–16806
32. Ting, Y. K., Morikawa, K., Kurata, Y., Li, P., Bahrudin, U., Mizuta, E., Kato, M., Miake, J., Yamamoto, Y., Yoshida, A., Murata, M., Inoue, T., Nakai, A., Shiota, G., Higaki, K., Nanba, E., Ninomiya, H., Shirayoshi, Y., and Hisatome, I. (2011) Transcriptional activation of the anchoring protein SAP97 by heat shock factor (HSF)-1 stabilizes K(v) 1.5 channels in HL-1 cells. *Br. J. Pharmacol.* **162,** 1832–1842
33. Wang, D., and Cotter, R. J. (2005) Approach for determining protein ubiquitination sites by MALDI-TOF mass spectrometry. *Anal. Chem.* **77,** 1458–1466
34. Song, B. L., Sever, N., and DeBose-Boyd, R. A. (2005) Gp78, a membrane-anchored ubiquitin ligase, associates with Insig-1 and couples sterol-regulated ubiquitination to degradation of HMG-CoA reductase. *Mol. Cell* **19,** 829–840
35. Pipalia, N. H., Cosner, C. C., Huang, A., Chatterjee, A., Bourbon, P., Farley, N., Helquist, P., Wiest, O., and Maxfield, F. R. (2011) Histone deacetylase inhibitor treatment dramatically reduces cholesterol accumulation in Niemann-Pick type C1 mutant human fibroblasts. *Proc. Natl. Acad. Sci. U.S.A.* **108,** 5620–5625
36. Munkacsi, A. B., Chen, F. W., Brinkman, M. A., Higaki, K., Gutiérrez, G. D., Chaudhari, J., Layer, J. V., Tong, A., Bard, M., Boone, C., Ioannou, Y. A., and Sturley, S. L. (2011) An "exacerbate-reverse" strategy in yeast identifies histone deacetylase inhibition as a correction for cholesterol and sphingolipid transport defects in human Niemann-Pick type C disease. *J. Biol. Chem.* **286,** 23842–23851
37. Scroggins, B. T., Robzyk, K., Wang, D., Marcu, M. G., Tsutsumi, S., Beebe, K., Cotter, R. J., Felts, S., Toft, D., Karnitz, L., Rosen, N., and Neckers, L. (2007) An acetylation site in the middle domain of Hsp90 regulates chaperone function. *Mol. Cell* **25,** 151–159
38. Hutt, D. M., Herman, D., Rodrigues, A. P., Noel, S., Pilewski, J. M., Matteson, J., Hoch, B., Kellner, W., Kelly, J. W., Schmidt, A., Thomas, P. J., Matsumura, Y., Skach, W. R., Gentzsch, M., Riordan, J. R., Sorscher, E. J., Okiyoneda, T., Yates, J. R., 3rd, Lukacs, G. L., Frizzell, R. A., Manning, G., Gottesfeld, J. M., and Balch, W. E. (2010) Reduced histone deacetylase 7 activity restores function to misfolded CFTR in cystic fibrosis. *Nat. Chem. Biol.* **6,** 25–33